Self-Assembly of Vertically Aligned Nanorod Supercrystals using HOPG

S. Ahmed and Kevin M. Ryan*

Materials and Surface Science Institute and Department of Chemistry and Environmental Sciences,

University of Limerick, Limerick, Ireland

RECEIVED DATE (to be automatically inserted after your manuscript is accepted if required according to the journal that you are submitting your paper to)

*To whom correspondence should be addressed . Email: kevin.m.ryan@ul.ie

ABSTRACT

Supercrystallisation of CdS nanorods (10 nm × 25 nm) into perpendicular superlattices was obtained by controlled evaporation of a nanorod solution trapped between a smooth substrate and a block of highly ordered pyrolytic graphite (HOPG). Hexagonal oriented domains, 2 μm^2 in size were routinely obtained on a variety of substrates without external electric fields.

Assembled one-dimensional (1D) nanocrystals have significant potential in a wide range of device applications such as in semiconductor electronics, data storage and third-generation solar-cells. [1-5] Finding methods to organise functional assemblies whose properties depend on the precise placement of anisotropic components remains a key challenge. Columnar 1D nanocrystals or nanorods primarily adopt assemblies parallel to substrates on deposition with nanorod aggregation influenced by dipolar attraction.[6, 7] Nanorod assembly with axial alignment perpendicular to the substrate is the desired geometry of most interest in key nanoelectronic, nanomagnetic and nanophotonic applications. For example, in semiconductor architectures, nanorod ensembles allow for potential miniaturization significantly beyond the lithographic limit.[8] Spherical, columnar and branched nanocrystals have been shown to exhibit single electron transistor behaviour.[9-11] Vertical alignment of semiconductor nanorods in an organised assembly would potentially allow each rod (single electron transitor) in a 2D array to be contacted individually at the end facet for macroscopic integration at < 5 nm separation. Self assembled computer memory based on vertical aligned magnetic nanorod arrays are also sought as the magnetic coercivity (Hc) can be controlled along the nanorod length.[12-14] In third generation solar-cells, anisotropic CdSe and CdTe nanocrystals have found significant application due to charge direction along the nanorod axis.[2, 3] Vertical alignment and close packing of CdSe and CdTe nanorods into 2D and 3D superlattices is desired to increase the power conversion efficiences of these devices. Orientation perpendicular to the electrodes is predicted to provide directed paths for electron and hole transfer to the electrodes whereas more efficient charge separation is achievable at the close packed nanorod/nanorod interface compared to that achievable in random rod assemblies.

Spherical nanocrystal assembly is well understood with face centred cubic ordered superlattices demonstrated for a wide range of nanocrystals with particle size dispersity less than 13%.[15-19] In contrast, independent assembly of 1D nanocrystals into vertically aligned arrays is greatly hindered by their anisotropy and increases in difficulty with increasing aspect ratio. Orientational order in nanorod solutions is possible and Li et al showed that surfactant passivated nanorods can form smectic or

nematic liquid crystalline phases if sufficiently monodisperse.[20] Drying of such a dispersion results in the aggregation into a nanorod solid with parallel to perpendicular orientation over hundreds of nanorod layers from edge to centre.[21] More controlled assembly of discrete anisotropic nanocrystals in a monolayer has required external electric fields to orientate the nanorod during packing. Very recently, Ryan et al and Russell et al. independently described the use of electric fields to assist the assembly of semiconductor nanorods into perpendicular superlattices.[22, 23] The electric field acts to orientate the nanorod dipole perpendicular to the field direction whereas either solvent evaporation or polymer phase separation can direct the position of the anisotropic nanocrystal. This directed assembly mechanism allows the formation of hexagonally ordered 2D supercrystals with axial orientation of the nanorods perpendicular to the substrate.

This paper reports the supercrytalline self-assembly as opposed to electric field directed assembly of CdS nanorods (10 nm × 25 nm) into large vertically aligned monolayers (2 μm^2) using highly ordered pyrolytic graphite (HOPG).

The CdS nanorods in this study were synthesised using the pyrolysis route[24], re-dispersed in a toluene solution and trapped between a block of highly ordered pyrolytic graphite (20 mm × 20 mm × 1mm, SPI Supplies) and a gold coated silicon wafer (rms roughness ~ 0.8 nm) as shown in figure 1. The solution was allowed to dry over several hours under controlled evaporation conditions. After removing the HOPG, high resolution scanning electron microscopy analysis (Hitachi S-4800), figure 2, showed monolayer domains as large as 2 μm^2 of perpendicularly oriented nanorods. This top-down view shows the upper hexagonally faceted (0001) crystal faces of the nanorods repeating in a close packed supercrystal. The domain shown is predominantly defect free with a very low concentration of nanorod vacancies. Some cracks are observable, the largest of which is 10 nm in width, resulting from yielding of the supercrystal due to the stress developed during toluene evaporation. The bright/dark contrast in the image mirrors the localised size variations of the gold supporting surface with smaller bright regions

3

owing to charging effect from residual phosphonic acid surfactants. The upper right and left edges of the supercrystal respectively, figure 2b and figure 2c, show that the nanorods are vertically aligned along the outer edge. This is an important result in anisotropic nanocrystal assembly as in previous reports, nanorod aggregation in the absence of electric fields showed successive parallel to perpendicular orientation from the edge to the centre of the domain. The mechanism of assembly in this study (figure 2) is not thought to be evaporation induced aggregation but supercrystal growth where incoming nanorods find their preferred location on the growing supercrystal face.

Figure 2d offers further evidence for perpendicular alignment at the domain edge as in this selected domain, the supercrystal edge is partially tilted providing a cross-section profile. The nanorod length measured from this supercrystalline arrangement is 25 nm, corresponding exactly to the length as measured under HRSEM from an isolated area of parallel rods (figure 2e).

Figure 2f and further magnified in figure 2g elucidates the defect free close packing in the centre of the domain. At these magnifications, the hexagonal shape of the wurtzite CdS nanorod as viewed along its [0001] axis is clearly visible with orientational alignment along the nanocrystalline facets across the nanorod-surfactant-nanorod interface apparent.

Transmission electron microscopy (TEM) sample preparation was carried out using a similar approach to the HRSEM study. A solution of nanorods was trapped between a HOPG block and a carbon coated nickel TEM grid. Perpendicularly aligned nanorod domains were predominantly found at the edges of the nickel mesh whereas on the gold substrate the domains were randomly distributed. It is expected that the grain boundaries on the gold surface provides regular heterogenous nucleation sites for supercrystal growth with nucleation on a TEM grid occurring at specific features along the metal grid bars. Figure 3a and 3b show selected images at increasing magnification of a perpendicular oriented nanorod supercrystal domain. The hexagonal faceted nanorods further pack into a superlattice with repeating

hexagonal geometry, as highlighted (A), that is almost defect free throughout. Close inspection reveals only a single nanorod vacancy (B) in this 480 nanorod section. Slight curvature in the TEM grid is responsible for some blurring at the outer edges that was further evidenced by eucentric high variations across the grid on continued investigation. Figure 3b clearly shows that the nanorods are azimuthally aligned along their respective crystal faces as previously observed in electric field assisted assembled rods offering further evidence for supercrystal growth. The nanorod diameter and internanorod repeat distance were calculated at ~ 10 nm and ~2 nm respectively from this image.

Small-angle x-ray scattering studies, figure 4, of dried nanorod solids in a quartz capillary correlated well to the internanorod repeat distances calculated from HRSEM and TEM images of the superlattice monolayer. Two reflections at $2\Theta = 0.417$ and 0.770 were obtained corresponding to diffraction from lattice repetition along the nanorod length (*l*) and across nanorod rows (*d*) over multilayers (Figure 4 inset schematic). The d-values corresponded to 22 nm and 11 nm respectively correlating to a nanorod length of 22 nm and an internanorod repeat distance of 13 nm ($2d/\sqrt{3}$). The SAXS study from the nanorod solids confirms the HRSEM and TEM (figure 4) observations that perpendicular nanorods in these assemblies are extraordinarily close-packed. The space occupied by the interdigitated phosphonic acid surfactants is considerably less than that previously reported for electric field aligned CdS nanorods which at 5 nm in diameter and at 3 nm separation were more loosely bound.

High resolution images in figure 5a clearly show atomic lattice fringing from the surface of the wurtzite nanorods. The lattice parameter was calculated from the further magnified image, figure 5 b, at 0.36 nm corresponding to the (100) reflection. Close analysis of the nanorods reveals slight angular variation in the direction of this (100) lattice fringing from rod to rod across the interdigitated surfactant interface of ± 6 degrees (figure 5b). This was confirmed by single crystal electron diffraction indexed in figure 5c. The single electron diffraction pattern, figure 5d, corresponds to a hexagonally close packed (hcp) wurtzite nanocrystal crystal observed in the [001] beam direction. The elongation of the spots

corresponding to reflections from the (100), (110) and (011) planes is consistent with the angular rotation of the nanorods observed in the lattice fringing. This angular variation is significantly less than the 60 degree rotation about the nanorod c-axis required for complete misalignment of crystal facets between neighbouring rods. A single nanorod highlighted in figure 5c on the edge of the nanocrystal superlattice does shows a 60 degree rotation in the 100 lattice fringe direction suggesting the misalignment of a 110 or 011 facet with the 100 facet in the neighbouring rod. Continued assembly along this edge would result in the emergence of a supercrystal stacking fault. Overall, the concentration of such stacking faults is low and azimuthal alignment from nanorod to nanorod of ± 6 degrees is conformal across a large selection of nanorod domains studied.

The extraordinary anisotropic nanorod assembly demonstrated in this work without applied fields is thought to occur predominantly by supercrystal growth. This we account for by several factors. Most important is the size monodispersity of the nanorods at < 5 % in length and diameter. The importance of size monodispersity in diameter to spherical supercrystal assembly is well known and in nanorod assembly, similar dimensional control in length is prerequisite. This was confirmed where syntheses with a significant polydispersity in nanorod length did not show any propensity for perpendicular self-assembly. The perfect hexagonal faceting along the c-axis of the wurtzite nanorods is of further importance to supercrystal growth. This is particularly evident with preferential azimuthal alignment along the (100) and (110) and (011) facets across the interdigitated surfactant interface. In the assemblies shown in figure 5, where atomic rows are uniform from rod to rod, each incoming nanorod needs to dynamically adjoin and disjoin for this correct orientation to be obtained. Allowing for the surfactant boundary, attaining the thermodynamic favourability necessitated by the correct orientation is only possible with extremely slow evaporation. This was confirmed where nanorods dropcast from solution without HOPG showed some parallel to perpendicular disorder from the edge to the centre (HRSEM image, supporting information). The rapid drying of the nanorods in this case induces nanorod aggregation as opposed to supercrystallisation.

The suggested influence of the HOPG substrate is related to its cleaved surface. Although it is atomically smooth, it cleaves randomly forming stepped surfaces at micron separation. The nanorod/ toluene solution trapped between the HOPG and a smooth surface e.g (gold coated silicon wafer) is therefore trapped in a very narrow capillary that facilitates slow evaporation. This slow evaporation allows attachment of solution dispersed nanorods to the growing crystal face on a timescale that allows the preferred orientation to be obtained.

The aspect ratio of the CdS nanorods is also thought to be influential in the observed self-assembly. In this study the nanorods have an aspect ratio of 2.5 (10 nm × 25 nm) whereas the CdS nanorods in the electric field assembly approach had an aspect ratio of 6 (5 × 30 nm).[18]   As the aspect ratio increases, three dimensional orientation of the nanorod necessary for dynamic growth is expected to be increasingly hindered by the end over end rotation needed for perpendicular rod attachment. In longer rods, electric field assisted assembly will present the rod to the growing crystal face in the preferred axial orientation and only rotation about this axis is required for azimuthal alignment to the correct facets. A complete study correlating assembly to the aspect ratio of nanorods, the presence or absence of an electric field and evaporation control to conclusively prove this hypothesis is currently under investigation and will be presented in future correspondence.

This research, to the best of our knowledge is the first report of perpendicular nanorod self assembly over large micron sized areas without external fields. The remarkable facet specific alignment from nanorod to nanorod across the surfactant boundary is clear evidence that assembly in this study is supercrystallisation driven. The extension of this assembly process to a diverse range of anisotropic nanoscale building blocks is certainly achievable and is predicated on size monodispersity and nanocrystalline geometry.
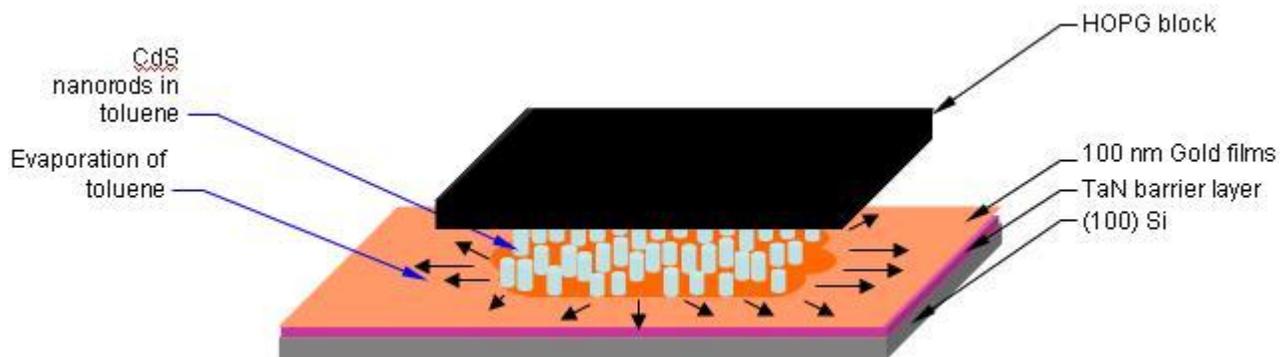
Figure 1. The 3D schematic shows the set-up used for monolayer nanorod assembly. A nanorod toluene solution was trapped between the gold sputtered substrate (Si / TaN /Au, 0.5 mm / 40 nm / 100 nm) and a highly ordered pyrolitic graphite block (HOPG, 20 mm × 20 mm × 1 mm, SPI Supplies) and allowed to dry over several hours under controlled evaporation conditions.
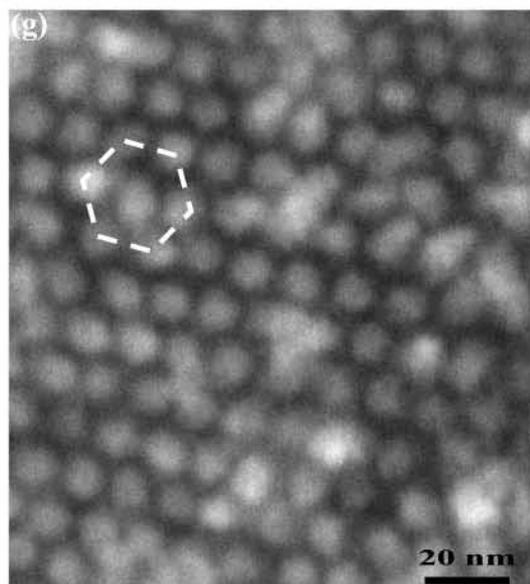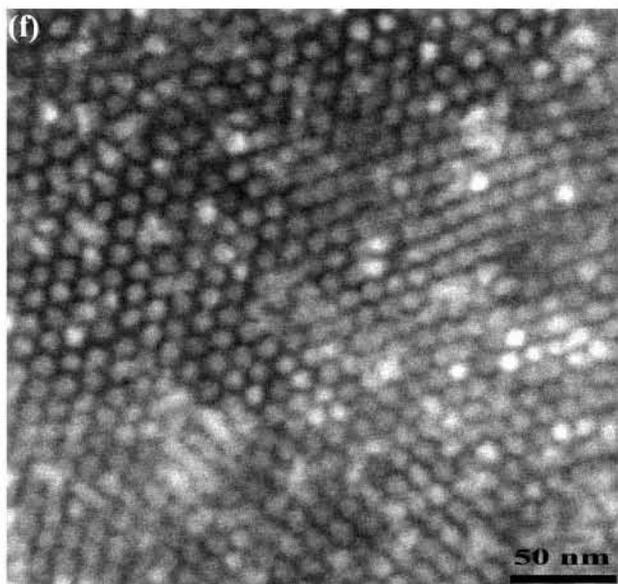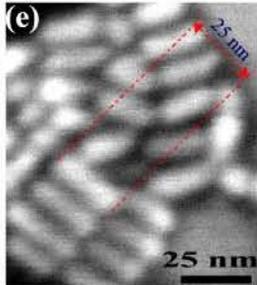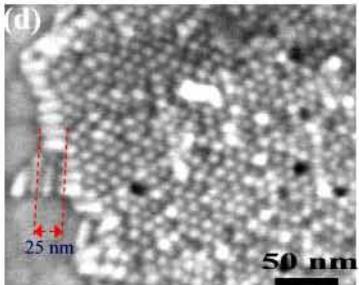
(a) 200 nm

(b) 100 nm

(c) 25 nm

(d) 25 nm 50 nm

(e) 25 nm 25 nm

(f) 50 nm

(g) 20 nm
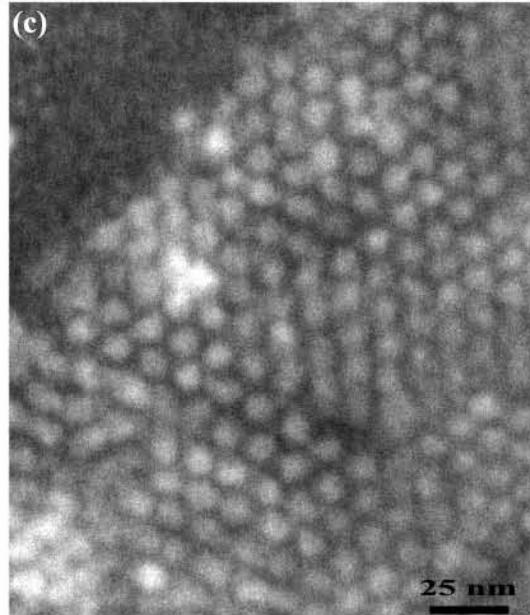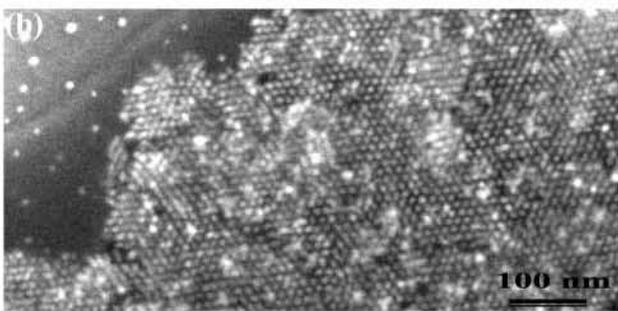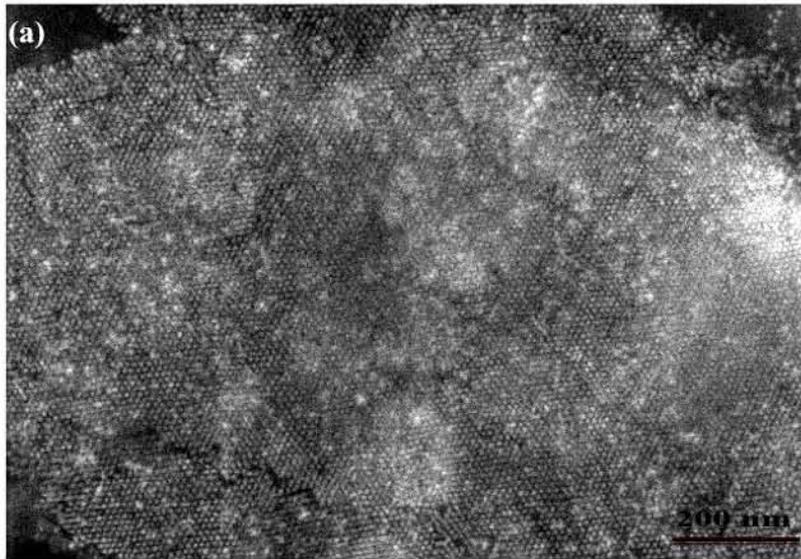
Figure 2. HRSEM images of a typical perpendicularly aligned nanorod superlattice: (a) Monolayer domain (2 μm^2) of perpendicularly oriented CdS nanorods (10 nm × 25 nm). (b) Magnified section showing the upper right edge of the domain (scale bar = 100 nm) (c) Magnified sections of the upper left edge (scale bar = 25 nm) (d) Partially tilted edge of CdS nanorod supercrystal providing cross-sectional view of vertically aligned 25 nm nanorods (scale bar = 50 nm). (e) Corresponding HRSEM image showing 25 nm nanorods parallel to the substrate (scale bar = 25 nm). (f) Magnified image from centre of supercrystal domain (scale bar = 50 nm). (g) Further magnified image from the centre of domain (scale bar = 20 nm), highlighted area shows hexagonal ordering.
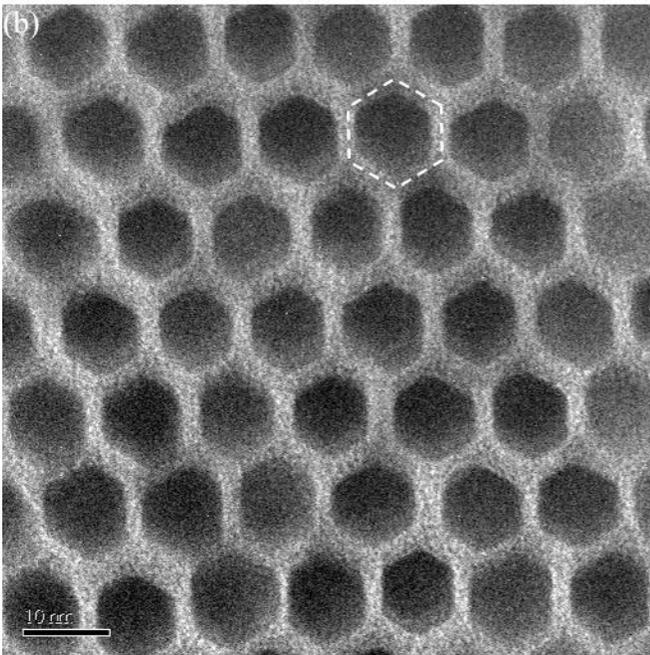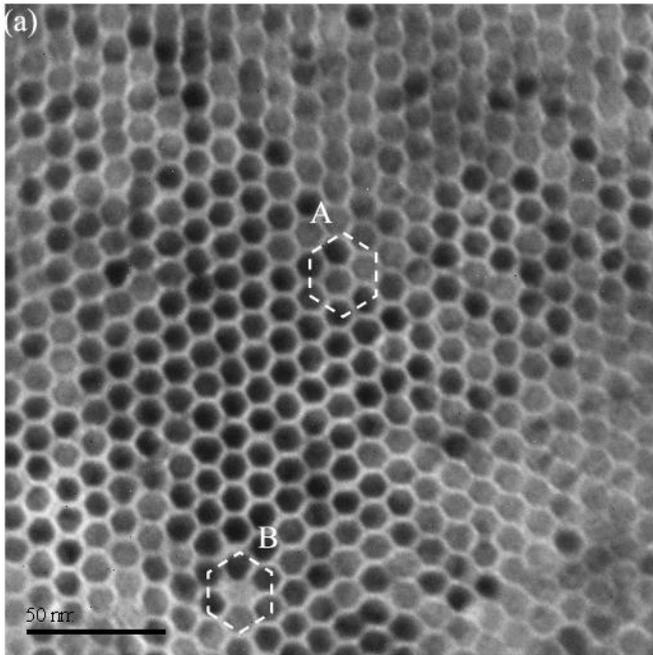
Figure 3. TEM images of perpendicularly aligned nanorod superlattice: (a) TEM image acquired from the centre of a domain (scale bar = 50 nm). Highlighted region A and B show repeating hexagonal geometry and nanorod vacancy respectively (b) Further magnified TEM image (scale bar = 10 nm), highlighted region shows perfect faceting of the wurtzite nanorod.
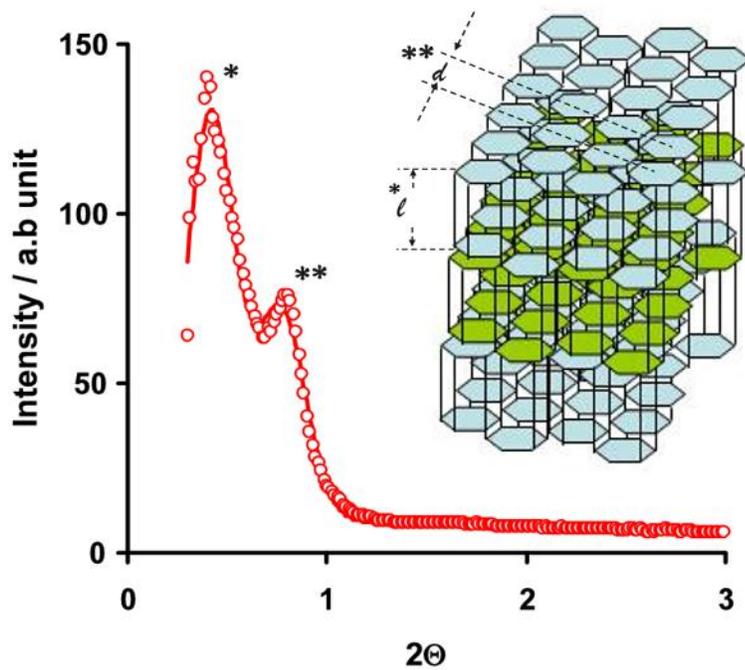
Figure 4. Plot of intensity (arbitrary unit) vs. 2Θ (degree) from small angle x-ray scattering (SAXS) data (curve fitted with correlation value R^2 = 0.994). Two reflections are indexed at 2Θ = 0.417 and 0.770 respectively corresponding to diffraction from lattice repetition along the nanorods length, *l* and across nanorod rows, *d* as shown in the inset schematic.
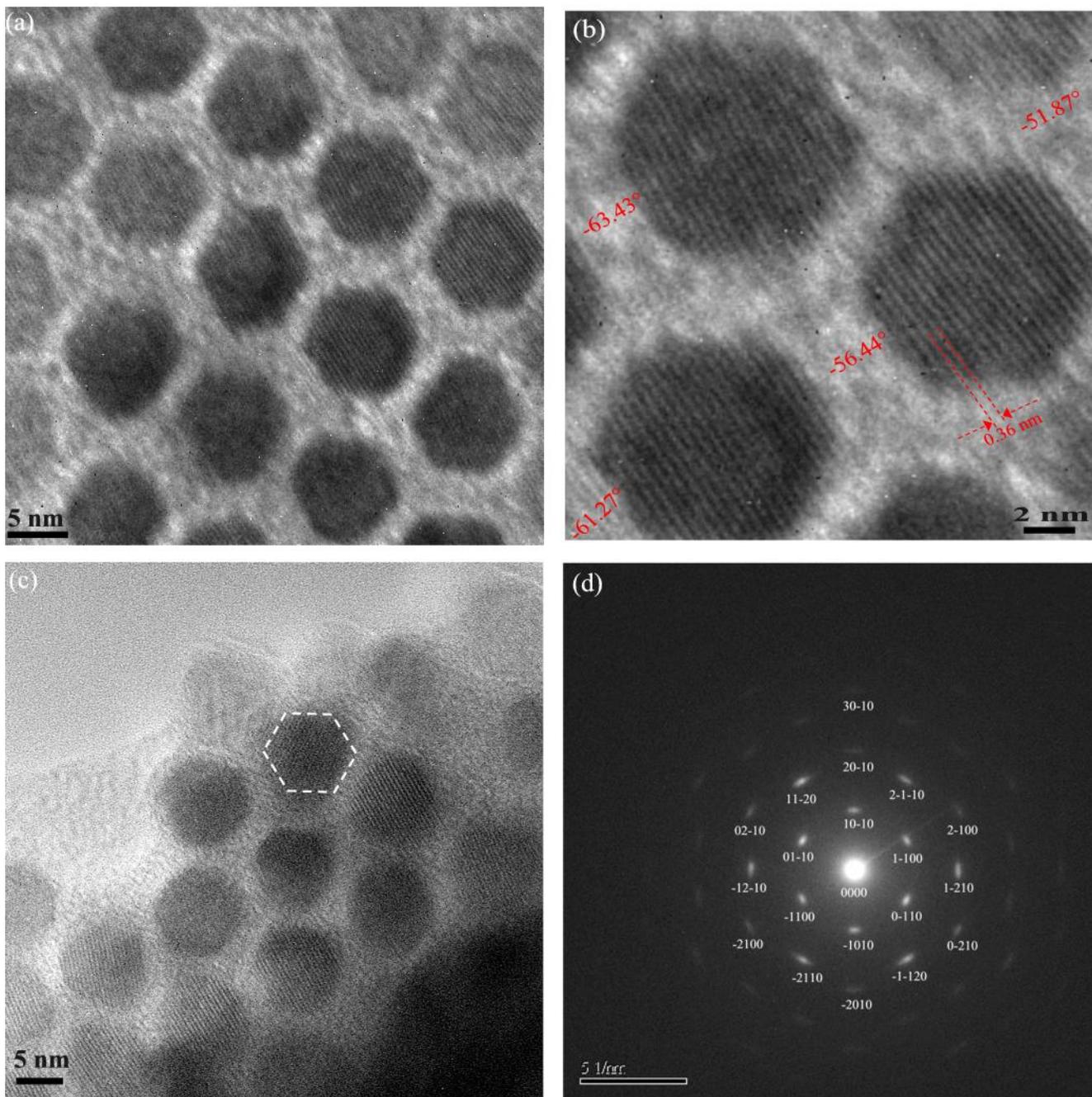
Figure 5. High resolution TEM images, acquired from the same domain as shown in figure 3 showing atomic lattice fringes and electron diffraction: (a) TEM image, acquired from the centre of figure 3a, shows lattice fringes from (100) planes of wurtzite CdS rods (scale bar = 5 nm). (b) Further magnified HRTEM image (scale bar = 2 nm) with an angular variation in lattice fringing of ± 6°. Highlighted lattice spacing of 0.36 nm is consistent with (100) planes of wurtzite CdS. (c) HRTEM image acquired from the edge of the domain shows large variation in angular rotation of the lattice fringes. (d) Single crystal electron diffraction indexing of CdS nanorods in the [0001] beam direction.

REFERENCES

1.   Appell, D. *Nature* **2002,** 419, 553-555.

2.   Gur, I.; Fromer, N. A.; Geier, M. L.; Alivisatos, A. P. *Science* **2005,** 310, 462-464.

3.   Huynh, W. U.; Dittmer, J. J.; Alivisatos, A. P. *Science* **2002,** 295, 2425-2427.

4.   Victor, F. P.; Kannan, M. K.; Paul, A. *Applied Physics Letters* **2001,** 78, (15), 2187-2189.

5.   Lieber, C. M. *MRS Bulletin* **2003**, 28, 486-491.

6.   Ghezelbash, A.; Koo, B.; Korgel, B. A. *Nano Lett.* **2006,** 6, (8), 1832-1836.

7.   Li, L.-S.; Alivisatos, A. P. *Adv. Mater.* **2003,** 15, 408-411.

8.   Ito, T.; Okazaki, S. *Nature* **2000,** 406, 1027-1031.

9.   Cui, Y.; Banin, U.; Bjork, M. T.; Alivisatos, A. P. *Nano Lett.* **2005**, 1519-1523.

10.   Gudiksen, M. S.; Maher, K. N.; Ouyang, L.; Park, H. *Nano Lett.* **2005,** 5, (11), 2257-2261.

11.   Klein, D. L.; Roth, R.; Lim, A. K. L.; Alivisatos, A. P.; McEuen, P. L. *Nature* **1997,** 389, 699-701.

12.   Park, J.-I.; Kang, N.-J.; Jun, Y.-W.; Oh, S. J.; Ri, H.-C.; Cheon, J. *ChemPhysChem* **2002,** 3, (6), 543-547.

13.   Richter, H. J.; Harkness IV, S. D. *MRS Bulletin* **2006,** 31, 384-388.

14.   Bennett, A. J.; Xu, J. M. *Applied Physics Letters* **2003,** 82, (19), 3304-3306.

15.   Courty, A.; Araspin, O.; Fermon, C.; Pileni, M. P. *Langmuir* **2001,** 17, (5), 1372-1380.

16.   Murray, C. B.; Kagan, C. R.; Bawendi, M. G. *Science* **1995,** 270, 1335-1338.

17.   Murray, C. B.; Kagan, C. R.; Bawendi, M. G. *Annu. Rev. Mater. Sci.* **2000,** 30, 545-610.

18.   Pileni, M. P. *J. Phys. Chem. B* **2001,** 105, 3358-3371.

19.   Pileni, M. P., *Nanocrystals Forming Mesoscopic Structures*. Wiley-VCH Verlag GmbH & Co. KGaA: Weinheim, 2005; p 330.

20.   Li, L.-S.; Walda, J.; Manna, L.; Alivisatos, A. P. *Nano Lett.* **2002,** 2, 557-560.

21.   Talapin, D. V.; Shevchenko, E. V.; Murray, C. B.; Kornowski, A.; Förster, S.; Weller, H. *J. Am. Chem. Soc.* **2004,** 126, 12984.

22.   Gupta, S.; Zhang, Q.; Emrick, T.; Russell, T. P. *Nano Lett.* **2006,** 6, (9), 2066-2069.

23.   Ryan, K. M.; Mastroianni, A.; Stancil, K. A.; Liu, H.; Alivisatos, A. P. *Nano Lett.* **2006,** 6, 1479-1482.

24.   Liu, H.; Owen, J. S.; Alivisatos, A. P. *J. Am. Chem. Soc.* **2007,** 129, (2), 305-312.

SUPPORTING INFORMATION PARAGRAPH

Supporting information shows a HRSEM image of nanorods dried in the absence of HOPG.

SYNOPSIS TOC